Available online at www.sciencedirect.com
ScienceDirect
Journal of Inorganic Biochemistry 101 (2007) 741–749
Journal of Inorganic Biochemistry
www.elsevier.com/locate/jinorgbio

Molecular structure, bioavailability and bioactivity of $[Cu(o\text{-phen})_2(cnge)](NO_3)_2 \cdot 2H_2O$ and $[Cu(o\text{-phen})(cnge)(H_2O)(NO_3)_2]$ complexes

Evelina G. Ferrer [a], Libertad L. López Tévez [b], Natalia Baeza [a], María J. Correa [a], Nora Okulik [b], Luis Lezama [c], Teófilo Rojo [c], Eduardo E. Castellano [d], Oscar E. Piro [e], Patricia A.M. Williams [a,*]

[a] Centro de Química Inorgánica (CEQUINOR), Facultad de Ciencias Exactas, Universidad Nacional de La Plata, C.C. 962, 1900 La Plata, Argentina
[b] Departamento de Química, Facultad de Agroindustrias, UNNE, Cte. Fernández 755, 3700 Pcia. R. Sáenz-Peña, Chaco, Argentina
[c] Departamento de Química Inorgánica, Facultad de Ciencia y Tecnología, Universidad del País Vasco, Apdo 644, 48080 Bilbao, Spain
[d] Instituto de Física de São Carlos, Universidade de São Paulo, C.P. 369, 13560 São Carlos (SP), Brazil
[e] Departamento de Física, Facultad de Ciencias Exactas, Universidad Nacional de La Plata and Instituto IFLP(CONICET), C.C. 67, 1900 La Plata, Argentina

Received 5 September 2006; received in revised form 20 December 2006
Available online 8 January 2007

Abstract

Two Cu(II) complexes with cyanoguanidine (cnge) and *o*-phenanthroline, $[Cu(o\text{-phen})_2(cnge)](NO_3)_2 \cdot 2H_2O$ (**1**) and $[Cu(o\text{-phen})(cnge)(H_2O)(NO_3)_2]$ (**2**), have been synthesized using different experimental techniques and characterized by elemental analyses, FTIR, diffuse and UV–vis spectra and EPR and magnetic moment measurements techniques. The crystal structures of both complexes were solved by X-ray diffraction methods. Complex (**1**) crystallizes in the monoclinic space group C2/c with $a = 12.621(5)$, $b = 31.968(3)$, $c = 15.39(1)$ Å, $\beta = 111.68(4)°$, and $Z = 8$ and complex (**2**) in the monoclinic space group $P2_1/n$ with $a = 10.245(1)$, $b = 13.923(2)$, $c = 12.391(2)$ Å, $\beta = 98.07(1)°$, and $Z = 4$. The environments of the copper(II) center are trigonal bipyramidal (TBP) for $[Cu(o\text{-phen})_2(cnge)]^{2+}$ and an elongated octahedron for $[Cu(o\text{-phen})(cnge)(H_2O)(NO_3)_2]$. Solution studies have been performed to determine the species distribution. The superoxide dismutase (SOD) activities of both complexes have also been tested in order to determine if these compounds mimic the enzymatic action of the enzyme SOD that protects cells against peroxide radicals.

Keywords: Copper complexes; Crystal structures; Superoxide dismutase activity; Species distribution

1. Introduction

Cyanoguanidine (or dicyandiamide, cnge) is the dimeric form of cyanamide, this compound being recently recognized as nitrogenase substrate. The dimer functions as a dehydration coupling agent that links glucose and adenosine to phosphoric acid and then forms glucose-6-phosphate and adenosine-5′-phosphate, respectively [1]. Despite its biological importance, cnge also has commercial applications as intermediate in the formation of pharmaceuticals, pesticides, fungicides, and various polymers. Cyanoguanidine is a planar molecule, which is able to coordinate transition metals [2–12] (see schema). The coordination preferentially occurs through the nitrile nitrogen N(1) and a secondary coordination through the imino nitrogen N(2) atom, as a bidentate bridging ligand. It has

* Corresponding author. Tel./fax: +54 0221 4259485.
E-mail address: williams@quimica.unlp.edu.ar (P.A.M. Williams).

0162-0134/$ - see front matter © 2007 Elsevier Inc. All rights reserved.
doi:10.1016/j.jinorgbio.2006.12.012

a completely delocalised π system behaving as a π-acceptor or σ-donor.

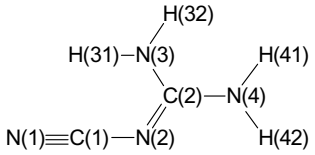

Some transition metal ions (cf. copper, platinum and nickel) are able to catalyze the addition of alcohols to the nitrile group in cnge, forming *n*-alkylguanylureas that coordinates the metal ions [13–16]. The formation of copper complexes of cyanoguanidine has been reported earlier, and they were structurally characterized. Some of the copper(II) complexes with nitrogenated ligands have been studied in connection with structural features such as hydrogen bonding interactions or important biological functions. Structural studies on the system copper(II)-cnge with a second ligand (2,2′-bipyridine, diethylenetriamine, 3-chloro-6-(pyrazol-1-yl)pyridazines [3,7–9]) have been carried out. The chemical speciation of an element, either essential or toxic, allows the knowledge of its bioavailability, transport and absorption properties in biofluids or tissues. It is then interesting to study the solution equilibrium of copper in the presence of these types of ligands. In order to understand the biological behavior of these kind of compounds we have undertaken a structural study of the compounds obtained using copper(II), cnge and *o*-phenanthroline. Two different complexes have been synthesized: $[Cu(cnge)(o\text{-phen})_2](NO_3)_2 \cdot 2H_2O$ (**1**) and $[Cu(cnge)(o\text{-phen})H_2O(NO_3)_2]$ (**2**). Their characterization has been performed by elemental analysis, X-ray diffraction, UV–visible, diffuse reflectance, FTIR and EPR spectroscopies and magnetic moment measurements. Due to the pharmacological interest of these copper–ligand systems, solution studies have been performed to determine the species distribution. The aim of this analysis is to obtain information about the bioavailability of these systems at different pH values (ionic strength 150 mM) and also to simulate naturally occurring mixtures of the metal ion and the ligands. Besides, it is demonstrated that some copper(II) complexes mimics the enzymatic action of the enzyme superoxide dismutase (SOD) that protects cells against peroxide radicals [17–21]. The SOD activities of both complexes have also been tested.

2. Experimental

2.1. Preparative

2.1.1. $[Cu(cnge)(o\text{-phen})_2](NO_3)_2 \cdot 2H_2O$ (1)

$Cu(NO_3)_2$ (1 mmol) was dissolved in warm water (2 mL). Aqueous cnge (5 mL) and ethanolic *o*-phenanthroline (2 mL) warm solutions were then added with stirring. The final molar ratio of Cu(II):cnge:*o*-phen was 1:2:2. The pH value was raised to 11 adding 1 M NaOH solution, and the solution was boiled about 10 min. The resulting green solution was set-aside at room temperature for crystallization. Green crystals adequate for crystallographic studies were obtained after two weeks. Anal. for $C_{26}H_{24}N_{10}O_8Cu$. Calcd. C%: 46.7, H%: 3.6, N%: 21.0. Exp. C%: 47.1, H%: 3.4, N%: 20.7. The value of the magnetic moment was 1.88 BM, indicating the presence of a single unpaired electron, as is expected for a d^9 ion.

2.1.2. $[Cu(cnge)(o\text{-phen})H_2O(NO_3)_2]$ (2)

The synthesis of the blue crystals of (**2**) has been performed like in (**1**), but the molar ratio was fixed in 1:1:1, with a final pH value of 5, at 30 °C. The resulting blue solution was set-aside at room temperature for crystallization. After three days, blue crystals suitable for X-ray measurements were obtained. Anal. for $C_{14}H_{14}N_8O_7Cu$. Calcd. C%: 35.8, H%: 3.0, N%: 23.8. Exp. C%: 36.0, H%: 2.9, N%: 23.9. The value of the magnetic moment was 1.85 BM indicating the same electronic configuration for copper(II) as in complex (**1**).

2.2. Reagents and instrumentation

All chemicals were of analytical grade and were used without further purification. Copper(II) nitrate trihydrate was purchased from Carlo Erba and cyanoguanidine and *o*-phenanthroline from Sigma.

IR spectra of powdered samples were measured with a Bruker IFS 66 FTIR-spectrophotometer from 4000 to 400 cm^{-1} in the form of pressed KBr pellets. Electronic absorption spectra were recorded on a Hewlett-Packard 8453 diode-array spectrophotometer, using 1 cm quartz cells. Diffuse reflectance spectra were registered with a Shimadzu UV-300 instrument, using MgO as an internal standard. Elemental analysis for carbon, hydrogen and nitrogen were performed using a Carlo Erba EA 1108 analyzer. A Bruker ESP300 spectrometer operating at X- and Q-bands and equipped with standard Oxford low temperature devices was used to record the spectra of the compounds at different temperatures. The magnetic field was measured with a Bruker BNM 200 gaussmeter, and the frequency inside the cavity was determined by using a Hewlett-Packard 5352B microwave frequency counter. EPR powder spectra of both compounds were recorded from 4.2 K to room temperature. A computer simulation of the EPR spectra was performed using the program SimFonia (WINEPR SimFonia v1.25, Bruker Analytische Messtecnik GmßH, 1996). Magnetic susceptibility measurements on polycrystalline samples were performed in the temperature range 5–300 K with a Quantum Design MPMS-7 SQUID magnetometer and using an applied field of 0.1 T. Diamagnetic corrections of the constituent atoms were estimated from Pascal's constants.

Table 1
Crystal data and structure solution methods and refinement results for [Cu(*o*-phen)$_2$(cnge)](NO$_3$)$_2$ · 2H$_2$O (**1**) and [Cu(*o*-phen)(cnge)(H$_2$O)(NO$_3$)$_2$] (**2**) complexes

	(**1**)	(**2**)
Empirical formula	$C_{26}H_{24}N_{10}O_8Cu$	$C_{14}H_{14}N_8O_7Cu$
Formula weight	668.09	469.87
Temperature (K)	293(2)	
Crystal system	Monoclinic	Monoclinic
Space group	*C*2/*c*	$P2_1/n$
Unit cell dimensions[a]		
a (Å)	12.621(5)	10.245(1)
b (Å)	31.968(3)	13.923(2)
c (Å)	15.39(1)	12.391(2)
β(°)	111.68(4)	98.07(1)
Volume (Å^3)	5771(5)	1750.0(4)
Z, calc. density (Mg/m^3)	8, 1.538	4, 1.783
Absorpt. coeff. (μ, mm^{-1})	1.661	2.343
F(000)	2744	956
Crystal size (mm)	0.25 × 0.25 × 0.16	0.20 × 0.20 × 0.20
Crystal color/shape	Green/fragment	Deep blue/spherical
Diffractometer/scan	CAD4/ω–2ϑ	CAD4/ω–2ϑ
Radiat., graph. Monochr. MoKα	$\lambda = 0.71073$ Å	CuKα, $\lambda = 1.54184$ Å
ϑ range for data coll.	2.76–67.02°	4.80–67.91°
Index ranges	$-14 \leqslant h \leqslant 15$, $0 \leqslant k \leqslant 28$, $-18 \leqslant l \leqslant 4$	$-12 \leqslant h \leqslant 12$, $0 \leqslant k \leqslant 16$, $0 \leqslant l \leqslant 14$
Reflections collected	6800	3340
Independent reflections	5113 [R(int) = 0.0151]	3188 [R(int) = 0.0363]
Completeness	99.1% (to $\vartheta = 67.02°$)	100.0% (to $\vartheta = 67.91°$)
Obs. reflects. [$I > 2\sigma(I)$]	3653	2793
Absorption correction	Multi-scan [22]	PLATON [23]
Max. and min. transm.	0.777 and 0.682	0.652 and 0.652
Data reduct. and correct.[b]	EXPRESS [24]	
and struct. solut.[c] and	SHELXS-97 [25]	
refinement[d] programs	SHELXL-97 [26]	
Refinement method	Full-matrix least-squares on F^2	
Weights, *w*	$[\sigma^2(F_o^2) + (0.097P)^2 + 1.24P]^{-1}$	$[\sigma^2(F_o^2) + (0.058P)^2 + 0.97P]^{-1}$
	$P = [\mathrm{Max}(F_o^2, 0) + 2F_c^2]/3$	
Data/restraints/param.	5113/4/434	3188/0/280
Goodness-of-fit on F^2	1.045	1.075
R-indices [$I > 2\sigma(I)$]	$R1 = 0.0497$, $wR2 = 0.1391$	$R1 = 0.0364$, $wR2 = 0.0970$
R-indices (all data)	$R1 = 0.0679$, $wR2 = 0.1622$	$R1 = 0.0422$, $wR2 = 0.1035$
Larg. peak and hole (eÅ^{-3})	0.288 and −0.343	0.526 and −0.353

R indices defined as: $R1 = \Sigma|F_o| - |F_c|/\Sigma|F_o|$, $wR2 = [\Sigma w(F_o^2 - F_c^2)^2/\Sigma w(F_o^2)^2]^{1/2}$.
[a] Least-squares refinement of $(\sin\vartheta/\lambda)^2$ values for 25(**1**) and 23(**2**) reflections in the $16.22° < \vartheta < 40.28°$ (**1**) and $17.89° < \vartheta < 39.58°$ (**2**) ranges.
[b] Corrections: Lorentz, polarization and absorption.
[c] Neutral scattering factors and anomalous dispersion corrections.
[d] Structure solved by direct and Fourier methods. The final molecular model obtained by anisotropic full-matrix least-squares refinement of the non-hydrogen atoms.

2.3. X-ray diffraction data

Crystal data, data collection procedure, structure determination methods and refinement results for both complexes are summarized in Table 1.

2.3.1. [Cu(o-phen)$_2$(cnge)](NO$_3$)$_2$ · 2H$_2$O

There are three different nitrate anions in the crystal. One of them is at a crystallographic general position, other on a twofold axis and a third one disordered at an inversion center. This latter ion was refined by fitting a rigid NO_3^- group with occupancy 1/2 to the corresponding residual electron density. There are three independent water molecules, one at a general position, other on a twofold axis and a third one disordered on an inversion center. The H-atoms of the first two water molecules were refined isotropically at their found positions with O–H distances restrained to a target value of 0.86(1) Å. The hydrogen atoms of the organic ligands were positioned stereo chemically and refined with the riding method.

2.3.2. [Cu(o-phen)(cnge)(H$_2$O)(NO$_3$)$_2$]

The H-atoms of the organic ligands were refined as described above. The water hydrogen atoms were located in a difference Fourier map and refined isotropically at their found positions.

2.4. Potentiometric titrations

The titrations were carried out at 298 K by coupling the titration cell with a thermostatic bath set at this temperature. Ionic strength was fitted at 0.150 M with NaCl in

the solutions, under nitrogen atmosphere. A Schott Gerate TS165 pH meter was used for EMF measurements and the added volumes were measured using a Techware (Sigma) Digitrate (25 mL). Volumes of titrated aliquots were always 25 mL. NaCl was dried until constant weight and stored in a desiccator. All solutions were prepared prior to their use with freshly, deionized and carbonate-free tridistilled water which was cooled under a constant flow of nitrogen. Diluted solutions of HCl (Merck p.a.) were standardized against TRISMA-base (hydroxymethyl aminomethane). Diluted NaOH solutions were prepared from a saturated NaOH solution and standardized against the HCl. The glass electrode was calibrated separately in a solution with known $[H^+]$ before and after each titration. Copper(II) solutions were prepared by dissolving $CuCl_2 \cdot 2H_2O$ (Merck) and were standardized using EDTA [27]. The data were collected from the lowest pH which could be reached in the experiment up to pH 12. Different metal–ligand ratios were selected in order to prevent precipitation.

2.5. SOD assays

The superoxide dismutase activity was examined indirectly using the nitroblue tetrazolium (NBT) assay. The indirect determination of the activity of SOD and the copper complexes was assayed by their ability to inhibit the reduction of NBT by the superoxide anion generated by the system xanthine/xanthine oxidase, at pH 10.2 (carbonate buffer), reported previously [28,29]. As the reaction proceeds, the formazan color was developed and it was observed a change from yellow to blue which was associated with an increase in the absorption spectrum at 560 nm. The reaction system contained different concentrations of the native SOD from bovine erythrocytes or the copper complex. The reaction was started by the xanthine–xanthine oxidase system in a concentration needed to yield the absorbance change between 0.2 and 0.4. Copper(II) chloride aqueous solution, 0.2 mM, was added in order to stop the NBT reduction. Free copper(II) ion is able to interact with the superoxide anion producing its dismutation. Ethylenediaminetetraacetic acid (EDTA), 0.1 mM, was included due to the formation of a copper chelate (CuEDTA) that has no SOD activity. Each experiment was performed in triplicate and at least three independent experiments were performed in each case. All the reagents (Sigma) were used as purchased. The amount of complex (or SOD) that gives a 50% inhibition (IC_{50}) was obtained by plotting the percentage of inhibition versus the log of the concentration of the tested solution.

3. Results and discussion

3.1. Crystallographical data

Intra-molecular bond distances and angles around copper(II) ion are given in Table 2. Figs. 1 and 2 are ORTEP [30] drawings of the complexes.

Table 2
Interatomic bond distances (Å) and angles (°) around copper in [Cu(*o*-phen)$_2$(cnge)](NO$_3$)$_2 \cdot 2H_2O$ and [Cu(*o*-phen)(cnge)(H$_2$O)(NO$_3$)$_2$]

[Cu(*o*-phen)$_2$(cnge)] (NO$_3$)$_2 \cdot 2H_2O$		[Cu(*o*-phen)(cnge)(H$_2$O)(NO$_3$)$_2$]	
Bond distances		Bond distances	
Cu–N(12)	1.982(3)	Cu–N	1.945(2)
Cu–N(21)	2.001(2)	Cu–O(1W)	1.966(2)
Cu–N(1)	2.004(4)	Cu–N(2)	1.990(2)
Cu–N(22)	2.095(2)	Cu–N(1)	2.001(2)
Cu–N(11)	2.115(3)	Cu–O(73)	2.569(2)
		Cu–O(62)	2.831(2)
Bond angles		Bond angles	
N(12)–Cu–N(21)	173.7(1)	N–Cu–O(1W)	92.38(9)
N(12)–Cu–N(1)	95.9(1)	N–Cu–N(2)	171.48(8)
N(21)–Cu–N(1)	90.4(1)	O(1W)–Cu–N(2)	91.81(8)
N(12)–Cu–N(22)	95.8(1)	N–Cu–N(1)	93.05(8)
N(21)–Cu–N(22)	80.6(1)	O(1W)–Cu–N(1)	174.38(8)
N(1)–Cu–N(22)	121.3(1)	N(2)–Cu–N(1)	82.62(8)
N(12)–Cu–N(11)	80.9(1)	N–Cu–O(73)	100.85(8)
N(21)–Cu–N(11)	96.0(1)	O(1W)–Cu–O(73)	89.92(8)
N(1)–Cu–N(11)	122.2(1)	N(2)–Cu–O(73)	86.56(7)
N(22)–Cu–N(11)	116.4(1)	N(1)–Cu–O(73)	90.47(7)
		N–Cu–O(62)	95.20(8)
		O(1W)–Cu–O(62)	91.10(8)
		N(2)–Cu–O(62)	77.31(6)
		N(1)–Cu–O(62)	86.97(7)
		O(73)–Cu–O(62)	163.86(6)

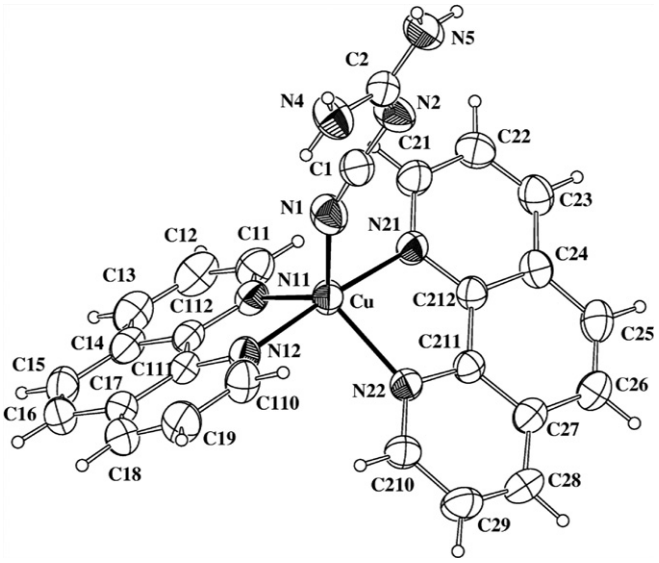

Fig. 1. View of the copper (II) complex in the [Cu(*o*-phen)$_2$(cnge)](NO$_3$)$_2 \cdot 2H_2O$ solid showing the labels of the non-H atoms and their displacement ellipsoids at the 30% probability level. Copper–ligand bonds are indicated by full lines.

3.1.1. [Cu(*o*-phen)$_2$(cnge)](NO$_3$)$_2 \cdot 2H_2O$ (**1**)

The copper(II) ion is in a trigonal bipyramidal environment, coordinated to two *o*-phenanthroline groups acting as bidentate ligands through their N-atoms [Cu–N bond distances in the range from 1.982(2) to 2.115(2) Å] and to the cyanide N-atom of a cyanoguanidine molecule [*d*(Cu–N) = 2.004(2) Å] that enters coordination with a bent Cu–N–N angle of 154.0(3)°.

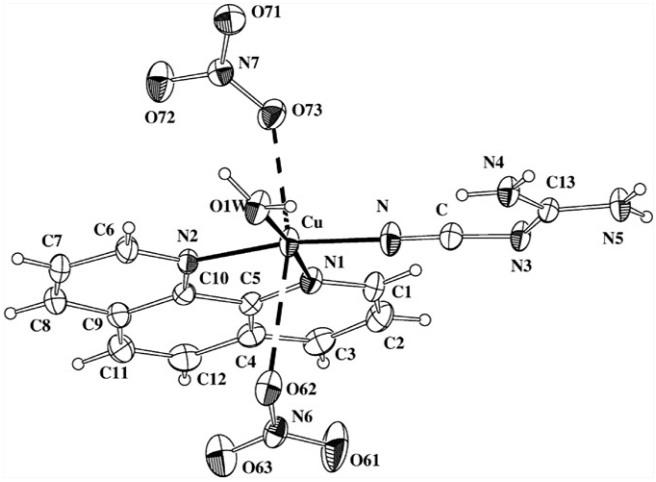

Fig. 2. Molecular plot of the [Cu(*o*-phen)(cnge)(H_2O)(NO_3)$_2$] complex. Copper–nitrate contacts are shown by dashed lines.

The crystals are further stabilized by a net of medium to strong intermolecular N–H ··· O bonds involving as donor the NH_2 terminal groups of the cyanoguanidine ligand and as acceptors the nitrate ion at the general position and the crystallization water molecules O2w and O3w. These H-bonds are detailed in the supplementary Table S1.

3.1.2. [Cu(o-phen)(cnge)(H_2O)(NO_3)$_2$] (2)

The metal ion is at the center of a strongly elongated octahedral environment, equatorially coordinated to a *o*-phenanthroline ligand through its N-atoms [Cu–N bond lengths of 1.990(2) and 2.001(2) Å] , to the cyanide N-atom of a cyanoguanidine molecule [*d*(Cu–N) = 1.945(2) Å] that enters coordination radially [∠(Cu–N–C) = 177.6(2)°] and to a water molecule along the oxygen electron lone pair [*d*(Cu–Ow) = 1.966(2) Å]. The distorted octahedral coordination around copper is completed with two nitrate ions at the axial positions [Cu ··· O contact distances of 2.569(2) and 2.831(2) Å]. The Cu ··· O(nitrate) contacts occurs along the oxygen electron lone pair [Cu ··· O–N angles of 126.3(2)° and 112.3(2)°].

The lattice is further stabilized by a network of intermolecular N–H ··· O(nitrate), N–H ··· N(cnge) and Ow–H ··· O(nitrate) bonds. These are detailed in the supplementary Table S2.

3.2. Infrared spectra

The major features in the IR spectra of the ligands upon coordination are related to the vibration modes of cnge and the nitrate anion. Strong *ν*(C≡N) bands are observed for cnge at 2212 and 2162 cm^{-1}. The shift of these bands in complex (**2**) to higher frequencies 2223–2184 cm^{-1} (with inversion of their intensities) is also observed when cyanide ion coordinates to a metal [7,31–33]. On the contrary, the coordination of cnge in complex (**1**) produces the opposite effect in the displacement of these bands (2180–2148 cm^{-1}) maintaining the same relationship in their relative intensities. In complex (**2**) cnge is strongly bonded in an octahedral environment with a very short Cu–N distance (1.945 Å) and larger coordinate angles Cu–N–C (177.6°). In complex (**1**), cnge is located in the base of a trigonal bipyramide with higher Cu–N distances (2.004 Å), and low coordinate Cu–N(1)–C(1) angles (154.0°), being weakly bonded to the metal.

Besides, in relation with the nitrate group, a diminution of the symmetry from D_{3h} in (**1**) to C_{2v} in (**2**) is inferred from the splitting of the ν_3(E′) band of nitrate anion (1380 cm^{-1}) that is observed at 1425 and 1377 cm^{-1}. The difference on these two values, $\Delta = 48$ cm^{-1}, is lower than that reported ($\Delta = 115$ cm^{-1}) [31] for a monodentate coordination of nitrate anion. Nevertheless, the tendency on the Δ value confirms the interaction of a single oxygen atom of nitrate anion with copper(II), in accord with the structural analysis. Furthermore, based on our spectroscopic data we have discarded a bidentate interaction of nitrate anion with the metal because in this case an even larger splitting of the bands ($\Delta = 186$ cm^{-1}) should be expected.

For both compounds, we have observed the characteristic *o*-phenanthroline bands located at 850 and 721 cm^{-1}.

3.3. EPR and magnetic properties

EPR powder spectra of both compounds as powder were recorded from 4.2 K to room temperature operating at X- and Q-band. Spin Hamiltonian parameters were estimated by comparison of the experimental spectra with those calculated at a second order of the perturbation theory with a computer simulation program (WINEPR-SimFonia, version 1.25, Bruker Analytische Messtechnik GmßH). The parameters were then optimised by the trial and error method. The overall appearance of all the registered spectra suggested an axially symmetry *g*-tensor for both copper(II) *o*-phenanthroline complexes, though there can be observed significant differences between them.

The thermal evolution of the X-band spectra of [Cu(*o*-phen)$_2$(cnge)](NO_3)$_2$ · 2H_2O (**1**) recorded on a polycrystalline sample is shown in Fig. 3. The room temperature spectrum is characteristic of an axial *g* tensor even if it is poorly resolved due to a rather large linewidth. When cooling down to 4.2 K the increase of the spin-lattice relaxation time causes a significant narrowing of the band and contributions from a hyperfine structure could be clearly detected on the low field region of the spectrum. Unfortunately, the resolution achieved at the lowest temperatures is not sufficient to enable us to fit the spectrum with an unambiguous solution.

The apparently axial symmetry of the *g*-tensor and the position of the perpendicular contribution ($g_\perp > 2.04$) suggest a $d_{x^2-y^2}$ ground state for the [CuN_5] cromophore in spite of the TBP topology deduced from the X-ray diffraction studies. However, it is to note that the axial appearance of many of the EPR spectra of TBP Cu(II) complexes may be not due to a small but important $d_{x^2-y^2}$ contribution that remains in the ground state, but

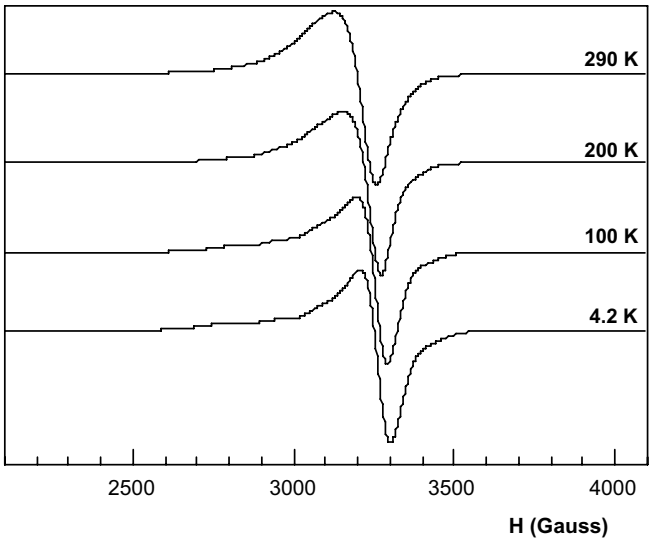

Fig. 3. Experimental X-band powder EPR spectra at 4.2, 100, 200 and 290 K of the complex $[Cu(o\text{-phen})_2(cnge)](NO_3)_2 \cdot 2H_2O$.

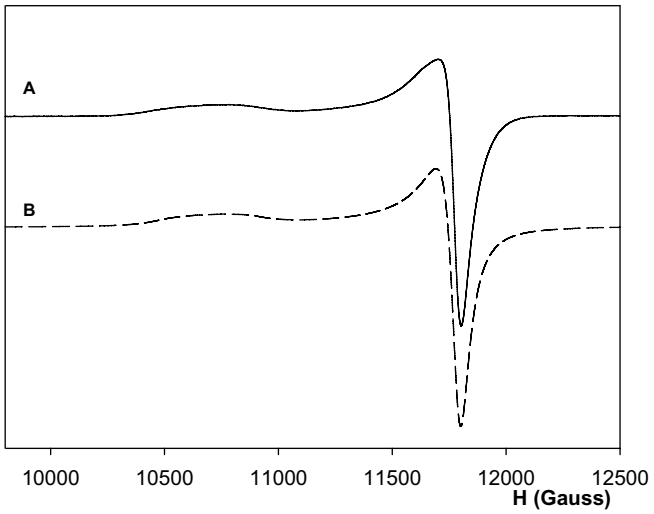

Fig. 4. Experimental (A) and simulated (B) Q-band powder EPR spectra at 290 K of the complex $[Cu(o\text{-phen})(cnge)(H_2O)(NO_3)_2]$.

to the metal d_{z^2} orbital contribution to vibronic effects that average the in-plane g and A values [34,35]. As in the usual Jahn–Teller effect, it appears that appropriate vibrational modes may be admitted to allow deviation from the d_{z^2} ground state that has been forced upon Cu(II) by constraining bidentate (*o*-phenanthroline) ligands. The crystal structure of complex **(1)** indicates some deviation of the 120° TBP geometry and it crystallizes in a $C2/c$ space group having a close similarity with other trigonal bipyramidal complexes [36]. For these kind of symmetries, the g values reflect better the large anisotropy in the equatorial plane of the trigonal bipyramidal, with $g_{\|}$ values higher than $g_{\perp}$ (as observed in complex (**1**)). The existence of a dynamic process is supported by the temperature dependence exhibited by the EPR spectra of complex (**1**), similar to that observed for nickel–ammonia complexes because of the development of higher effective symmetries at higher temperatures [37].

The best resolved resonance signal for the polycrystalline EPR of $[Cu(o\text{-phen})(cnge)(H_2O)(NO_3)_2]$ (**2**) is shown in the Fig. 4. EPR parameters deduced from the simulated spectrum obtained from the Q-band spectra (290 K) are $g_{\|} = 2.272$ and $g_{\perp} = 2.061$ being $A_{\|} = 140 \times 10^{-4}\ cm^{-1}$ and $A_{\perp} < 10 \times 10^{-4}\ cm^{-1}$. The sequence $g_{\|} > g_{\perp} > 2.04$ is consistent with a $d_{x^2-y^2}$ ground state as expected for an elongated octahedron. Moreover, the low $g_{\|}$ value is in good agreement with the strongly elongated octahedral environment for the Cu(II) ions observed in the structural analysis. As expected, the hyperfine coupling constant calculated for a parallel component is comparable to those found for complexes in which the copper(II) atom is coordinated to N- and O-atoms [38–41]. From our EPR parameters, there results a tetragonal distortion factor $f = g_{\|}/A_{\|} = 162$ cm (Blumberg–Peisach approach [42]) which lies in the range of copper(II) complexes with 3 N-atoms and 1 O-atom in the coordination sphere around the metal center.

Magnetic susceptibility measurements carried out between 4.2 K and room temperature have shown typical Curie–Weiss behavior for both compounds. The calculated Curie-constants are 0.440 and 0.428 cm^3 K/mol for complexes (**1**) and (**2**), respectively, corresponding to average g-values of 2.16 and 2.13 in good agreement with the EPR results. The Weiss temperature intercept is close to zero in both cases as indicating that the Cu(II) centers are practically isolated from the magnetic point of view, in accord with the detection of hyperfine structure in the EPR spectra.

3.4. Electronic spectra

Electronic UV–visible and diffuse reflectance spectra of the two complexes were measured (see Table 3). Diffuse reflectance spectra showed the characteristic broad bands for copper(II) complexes with Jahn–Teller tetragonally distorted octahedron, CuN_3O_3 chromophore, for complex (**2**) [43]. In complex (**1**) the transitions appeared in the expected range for a CuN_5 chromophore (trigonal bipyramid). The shift to the blue region with respect to the aqua complex of copper(II) bis(*o*-phenanthroline) is indicative of the substitution of the oxygen atom of the water molecule from the copper coordination sphere by the nitrogen donor atom of cnge [36]. Aqueous solution UV–visible spectra at pH 10.2

Table 3
Electron absorption and diffuse reflectance spectra of the two new complexes (Band positions in nm). ε, molar extinction coefficients in $M^{-1}\ cm^{-1}$ br, broad

	$[Cu(cnge)(o\text{-phen})H_2O(NO_3)_2]$ (**2**) blue	$[Cu(cnge)(o\text{-phen})_2](NO_3)_2 \cdot 2H_2O$ (**1**) green
Diffuse reflectance	650, 745 (br)	755 (br)
Aqueous solution, pH 10.2	668 $\varepsilon = 47.8$	672 $\varepsilon = 21.2$

displayed broad bands maximum at ca. 670 nm. As no appreciable changes occur in the position of very broad d–d bands upon dissolution of the complex (**2**), we conclude that there are not significant differences between the environment around the metal in the solid state and the solution. However, complex (**1**) may expand its coordination sphere upon dissolution, as suggested by the observed shift to the blue of the electronic band. The solution spectra consist of a broad band centered at ca. 670 nm and a shoulder on the low energy side. This broad band envelope contains the $d_{xy} \rightarrow d_{x^2-y^2}$ and $d_{xz,yz} \rightarrow d_{x^2-y^2}$ transitions. The third expected electronic transition in an approximate D_{4h} symmetry ($d_z^2 \rightarrow d_{x^2-y^2}$) occurs at lower energies. The position of the main peak of the broad band is located between the normal values observed for CuO_6 and CuN_6 chromophores (770 and 550 nm, respectively) [43].

3.5. Determination of acidity and stability constants

Synthetic chemistry indicated that the complexes [Cu(*o*-phen)$_2$(cnge)]$(NO_3)_2 \cdot 2H_2O$ and [Cu(*o*-phen)(cnge)-$(H_2O)(NO_3)_2$] could be successfully prepared in the micro-crystal forms in mixed water–organic solvent medium. However, it is doubtful that the same structures can also exist in the water solution. In order to get a better understanding of the behavior of the quaternary system, titration studies were undertaken.

For the determination of the acid dissociation constant of the ligands (LH = cngeH, and AH^+ = *o*-phenH^+), aqueous solutions of the protonated ligands were titrated in the absence of metal. The experimental $\log\beta_{0101}$ value of 5.0 for *o*-phenH^+ was recalculated and found in good agreement with the reported value [44,45]. To our knowledge the pKa value for cngeH has not been reported in the literature.

The stability constants of the ternary complexes were refined separately using the titration data of these systems, in the same conditions of temperature and ionic strength. They were fixed and consequently only quaternary species were refined in the final model. Sets of titrations with varying total concentrations and concentration ratios of the components were carried out to establish the equilibrium of the quaternary system Cu^{2+}/*o*-phen/cnge/H^+.

The formation constants denoted β_{pqrs} correspond to the general notation:

$$p\mathrm{Cu}^{2+} + q\text{-phen} + r\text{cnge} + s\mathrm{H}^+ \rightleftharpoons (\mathrm{Cu}^{2+})_p(\text{-phen})_q(\text{cnge})_r(\mathrm{H}^+)_s$$

A value of $pK_w = 13.76$ (corresponding to $\log\beta_{000-1} = -13.76$) was assumed for the experimental conditions ($T = 298$ K, $I = 150$ mM).

To determine the formation constants of the ternary (Cu^{2+}/*o*-phen/H^+ and Cu^{2+}/cnge/H^+) and quaternary (Cu^{2+}/*o*-phen/cnge/H^+) systems, data collected from several sets of titrations were analyzed with Best and SUPERQUAD calculation programs [46].

To fit potentiometric data with the SUPERQUAD program, different species were considered and the best model was refined. The stability constants ($\log\beta$), reported in Table 4 were used to compute the species distribution curve that is shown in Fig. 5 for 1:1:1 Cu/*o*-phen/cnge ratio.

As it can be seen from Fig. 5 the most striking feature of the copper/*o*-phen/cnge/H^+ system is that the percentage of free copper at low pH is negligible small. The complex formation reactions start earlier in strongly acidic solution (pH < 2) when stable mono and bis(ligand) complexes are formed. This behavior is in accord with the higher stabilities related to the chelated systems such as Cu/*o*-phen/H^+ [47] where $[CuA]^{2+}$, $[CuA_2]^{2+}$ and $[CuA_3]^{2+}$ are major species in this pH range. Moreover, $[CuLH]^{2+}$complex is also observed in acidic conditions and appears to be the dominant species for the ternary Cu/cnge/H^+ system, using equimolar quantities of copper and each ligand. On the other hand, upon varying the ratio of copper to ligand concentrations such as 1:3:1 (Cu(II):*o*-phen:cnge), CuA_3 moiety dominates the species diagram (data not shown).

Table 4
Composition, notation and formation constants (β) for the Cu^{2+}/cnge (L) and Cu^{2+}/*o*-phen(A)/cnge (L)/H^+ system (0.150 M NaCl, 298 K)

Species *pqrs*	Formula	Logβ
0011	AH^+	5.00
0101	LH	11.57
1100	$[CuA]^{2+}$	9.08
1200	$[CuA_2]^{2+}$	15.80
1300	$[CuA_3]^{2+}$	21.00
110−2	$[CuAH_{-2}]$	−9.90
1011	$[CuLH]^{2+}$	19.27
1022	$[CuL_2H_2]^{2+}$	34.06
1110	$[CuAL]^+$	19.03
1111	$[CuALH]^{2+}$	18.40
1210	$[CuA_2L]^+$	22.14

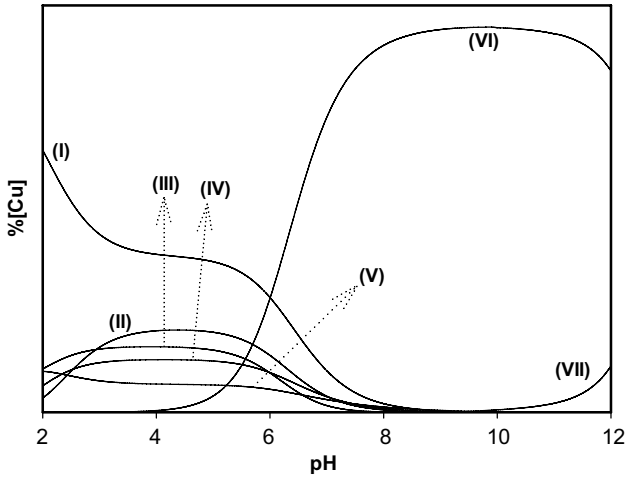

Fig. 5. Species distribution for the Cu^{2+}/*o*-phen/cnge/H^+ system. Total concentration Cu^{2+}: 1 mM, *o*-phen: 1 mM and cnge: 1 mM as a function of pH, 25 °C, $I = 0.150$ M NaCl. $[CuLH]^{2+}$ (I), $[CuA_3]^{2+}$ (II), $[CuL_2H_2]^{2+}$ (III), $[CuA_2]^{2+}$ (IV), $[CuA]^{2+}$ (V), $[CuAL]^+$ (VI), $[CuAH_{-2}]$ (VII).

Under the experimental conditions (1:1:1 ratio), the interaction of the ligands with the metal center occurs with the same donor groups, binding via the non charged (*o*-phen) or the protonated (cnge) N-atoms. The competition between the bis-ligand species, $[CuA_2]^{2+}$ and $[CuL_2H_2]^{2+}$ is observed from pH 2 up to 7.

Under the present experimental conditions, the increase of the pH value induces the formation of $[CuAL]^{+}$ that appears as the main species in the alkaline pH range. The concentration of the other quaternary species is almost negligible under the selected experimental conditions. As it can be seen from Fig. 5, the formation of (1,1,1,0)-species is favored in water solution on behalf of (1,1,1,1)-species. The displacement of the equilibrium and the release of a proton from $[CuALH]^{2+}$ complex can be explained by the possible deprotonation of a coordinated water molecule, producing an increase of the thermodynamic stability of the complex [48]. The presence of hydroxo species is also observed for $[CuAH_{-2}]$ complex at higher pH values. The species $[CuAL]^{+}$ also appears as the main event in neutral or alkaline pH range at the concentration range used for SOD determinations (50 μM). From pH 8.6 to 11.9 this species is practically the only one in the system (percentage distribution: 99%, data not shown).

Briefly, the potentiometric results account for the species distribution in water solutions at 25 °C. The formation of the solid and neutral $[Cu(o\text{-phen})(cnge)(H_2O)(NO_3)_2]$ complex at pH 6 in warm water-methanol medium (the conditions employed in the synthesis of the monocrystals) may be favored by the lower solubility of the neutral compound in these solvents. The synthesis of 1,2,1,1 species was performed at extreme conditions, namely at pH 11, different molar ratio of the reactants (1:2:2), a water–ethanol mixture as the solvent and at boiling temperature. The concentration of this species becomes negligible small when using the experimental conditions of the potentiometric studies. Besides, it has been determined that these solids were not stable in water solution, being transformed in the $[CuAL]^{+}$ cation upon dissolution in alkaline media and that behave in a similar manner in the other performed solution studies (electronic spectra and SOD activities measurements, see below).

3.6. Superoxide dismutase activity

Measurements of SOD-like activities are a good marker of the antioxidant properties of copper compounds. It has been reported that the presence of coordination sites belonging to nitrogen heteroaromatic rings such as imidazole, pyridine and pyrazole is important for high SOD activity [49]. Therefore, we have selected phenanthroline and another nitrogen containing ligand:cyanoguanidine to generate an active site similar to that of copper(II) in the native enzyme. The determinations were carried out using the xanthine/xanthine oxidase/NBT assay system. NBT acts as superoxide detecting agent through its reduction to methylformazan (MF^{+}). In the presence of the copper complex the mechanism of the reduction of NBT to MF^{+} comprises several reactions. The system xanthine/xanthine oxidase produces superoxide that reacts with NBT to produce MF^{+}. At the same time the copper complex interacts with $O_2^{\cdot-}$ catalyzing its dismutation to molecular oxygen and hydrogen peroxide; this reaction reduces the superoxide concentration in solution and, thus, the MF^{+} production rates (i.e., slowing down absorbance variation). The experimental determination of SOD activity was performed at pH 10.2 taking into account the presence of a single species in this region. Both complexes produced a similar 50% inhibition (IC_{50}) 40.7 ± 3.7 μM and 34.7 ± 5.3 μM, for complex (**2**) and complex (**1**), respectively. Under the present experimental conditions the IC_{50} value of SOD enzyme (from bovine erythrocytes) was 4 nM, similar to previously reported values [50].

If compounds have an IC_{50} value below 20 μM, they show SOD-like activity but they are inactive at higher concentrations. The experimental IC_{50} values obtained for complexes (**1**) and (**2**) were found to be in the lower limit of the active compounds [51] (sometimes called moderate behavior toward the dismutation of superoxide).

4. Conclusions

The synthesis and the attainment of rational control of new inorganic complexes is found to be a process influenced by subtle environmental changes. To achieve control over them lies at the very heart of crystal engineering. They may afford significant variations in chemical and physical properties as well as overall structures. In this paper we report the synthesis of two new complexes of Cu(II), cyanoguanidine and *o*-phenanthroline, obtained using different stoichiometric ratio of each reactant and temperature. Our results underline the importance of the appropriate choice of the experimental conditions (solvent, temperature, metal to ligand ratios) for the regulation of the composition of the metal complexes in the solid state. Besides, either in solution or in solid state, the stoichiometries of the copper(II) compounds may differ.

The behavior in biological fluids is governed by thermodynamic equilibrium, being the species distribution a powerful tool for the determination of the major species. The formation constants of each species, allows the determination of the fraction of the different copper containing species at a fixed pH value that depends again on the molar ratio of the reactants. On determining the distribution of the species of the Cu/*o*-phen/cnge/H^{+}system at 25 °C, physiological ionic strength and aqueous solution, it can be concluded that the more stable bioactive species are the quaternary species and at the selected experimental conditions, the species $[CuAL]^{+1}$(1,1,1,0) (hydroxo complex (**2**)) predominates at pH values higher than 7. The biological activities of both complexes have been determined by their ability in mimicking superoxidedismutase enzyme. The measured activity was of the same order of magnitude for the solution of both complexes at pH 10.2.

Acknowledgements

This work was supported by UNLP, CONICET, CICPBA, FAPESP of Brazil and Eusko Jaularitza/ Gobierno Vasco MV-2004-3-39. Part of the X-ray diffraction experiments were carried out at LANADI (CONICET-UNLP), Argentina. EGF, NO and OEP are members of the Carrera del Investigador, CONICET. PAMW is a member of the Carrera del Investigador CICPBA, Argentina.

Appendix A. Supplementary data

Listings of fractional coordinates and equivalent isotropic displacement parameters Tables S1 and S2, full bond distances and angles (Tables S3–S6), atomic anisotropic thermal parameters (Tables S7 and S8), hydrogen atoms positions (Tables S9 and S10), H-bonds distances and angles (Tables S11 and S12) and calculated for [Cu(*o*-phen)$_2$(cnge)] $(NO_3)_2 \cdot 2H_2O$ (**1**) and [Cu(*o*-phen)(cnge)-$(H_2O)(NO_3)_2$] (**2**). Supplementary data associated with this article can be found, in the online version, at doi:10.1016/j.jinorgbio.2006.12.012.

References

[1] A.J. Belsky, T.B. Brill, J. Phys. Chem. A 102 (1998) 4509–4516.
[2] U. Kolodziej, J. Przluski, Polyhedron 4 (1985) 395–399.
[3] A.S. Batsanov, P. Hubberstey, C.E. Russell, J. Chem. Soc., Dalton Trans. (1994) 3189–3190.
[4] M.J. Begley, O. Eisenstein, P. Hubberstey, S. Jackson, C.E. Russell, P.H. Walton, J. Chem. Soc., Dalton Trans. (1994) 1935–1942.
[5] J. Pickardt, B. Kühn, Z. Naturfosch. 51b (1996) 1701–1706.
[6] J. Pickardt, B. Kühn, Z. Naturfosch. 51b (1996) 1469–1472.
[7] A.S. Batsanov, P. Hubberstey, C.E. Russell, P.H. Walton, J. Chem. Soc., Dalton Trans. (1997) 2667–2672.
[8] M.J. Begley, P. Hubberstey, J. Stroud, Polyhedron 16 (1997) 805–813.
[9] A.J. Blake, P. Hubberstey, W. Li, C.E. Russell, B.J. Smith, L.D. Wraith, J. Chem. Soc., Dalton Trans. (1998) 647–655.
[10] L.M.D.R.S. Martins, J.J.R. Fraústo da Silva, A.J.R. Pombeiro, R.A. Henderson, D.J. Evans, F. Benetollo, G. Bombieri, R.A. Michelin, Inorg. Chim. Acta 291 (1999) 39–48.
[11] P.J. Bailey, S. Pace, Coord. Chem. Rev. 214 (2001) 91–141.
[12] M.K. Ammar, F.B. Amor, T. Jouini, A. Driss, J. Chem. Crystallogr. 32 (2002) 87–89.
[13] P. Ray, Chem. Rev. 61 (1960) 313–359.
[14] R.L. Dutta, A.M. Singh, J. Indian Chem. Soc. LII (1975) 1000–1001.
[15] W.K. Baker Jr., M. Daniels, J. Inorg. Nucl. Chem. 25 (1963) 1194–1196.
[16] P.A.M. Williams, E.G. Ferrer, N. Baeza, O.E. Piro, E.E. Castellano, E.J. Baran, Z. Anorg. Allg. Chem. 631 (2005) 1502–1506.
[17] Y. Tian, Y. Fang, C. Sun, W. Shen, Q. Luo, M. Shen, Biochem. Biophys. Res. Commun. 191 (1993) 646–653.
[18] A. Barik, B. Mishra, L. Shen, H. Mohan, R.M. Kadam, S. Dutta, H.Y. Zhang, K.I. Priyadarsini, Free Radic. Biol. Med. 39 (2005) 811–822.
[19] M. Gonzalez-Alvarez, G. Alzuet, J. Borras, L. del Castillo Agudo, S. Garcia-Granda, J:M: Montejo–Bernardo. Inorg. Chem. 12 (2005) 9424–9433.
[20] T. Fjuimori, S. Yamada, H. Yasui, H. Sakurai, Y. In, T. Ishida, J. Biol. Inorg. Chem. 10 (2005) 831–841.
[21] H. Liu, W. Wang, J. Zhang, X. Wang, Ecotoxicol. Environ. Saf. 65 (2006) 350–354.
[22] R.H. Blessing, Acta Cryst. A51 (1995) 33–38.
[23] PLATON, A Multipurpose Crystallographic Tool, Utrecht University, Utrecht, The Netherlands, Spek, A.L. 1998.
[24] CAD4 Express Software. Enraf-Nonius, Delft, The Netherlands, 1994.
[25] G.M. Sheldrick. SHELXS-97. Program for Crystal Structure Resolution. Univ. of Göttingen: Göttingen, Germany, 1997.
[26] G.M. Sheldrick. SHELXL-97. Program for Crystal Structures Analysis. Univ. of Göttingen: Göttingen, Germany, 1997.
[27] I.M. Kolthoff, E.B. Sandell, E.J. Meehan, S. Bruckenstein, Análisis Químico Cuantitativo, fifth ed., Librería y editorial Nigar, Buenos Aires, 1979.
[28] C. Beauchamp, I. Fridovich, Anal. Biochem. 44 (1971) 276–287.
[29] I. Iwamoto, I. Mifuchi, Chem. Pharm. Bull. 30 (1982) 237–241.
[30] C.K. Johnson, ORTEP. Report ORNL-3794, Oak Ridge, TN, 1965.
[31] K. Nakamoto, Infrared and Raman Spectra of Inorganic and Coordination Compounds, fourth ed., John Wiley, New York, 1986.
[32] L.A. Sheludyadova, E.V. Sobolev, A.V. Arbuznikov, E.B. Burgina, L.I. Kozhevina, J. Chem. Soc, Faraday Trans. 93 (1997) 1357–1360.
[33] M.J. Begley, P. Hubberstey, J. Chem. Res. (S) 1982 (1982) 118–119.
[34] G. Kokoszka, K.D. Karlin, F. Padula, J. Baranowski, C. Goldstein, Inorg. Chem. 23 (1984) 4378–4380.
[35] R. Barbucci, A. Bencini, D. Gatteschi, Inorg. Chem. 16 (1977) 2117–2120.
[36] A. Bencini, D. Gatteschi, Inorg. Chem. 16 (1977) 1994–1997.
[37] J. Stankowski, J.M. Janik, A. Dezor, B. Sczaniecki, Phys. Statu. Solidi. A 16 (1973) K167–K168.
[38] M. Jezowska-Bojczuk, W. Le'sniak, J. Inorg. Biochem. 85 (2001) 253–261.
[39] C.J. Williams, H. Morris, J. Svorec, M. Valkova, M. Valko, J. Moncol, M. Manzur, F. Valach, M. Melnik, J. Mol. Struct. 659 (2003) 53–60.
[40] A. Rockenbauer, T. Szabo-Planka, Z. Arkosi, L. Korecz, J. Am. Chem. Soc. 123 (2001) 7646–7654.
[41] J. Perkinson, S. Brodie, K. Yoon, K. Mosny, P.J. Carroll, T. Vance Morgan, S.J. Nieter Burgmayer, A. Rockenbauer, T. Szabó-Plánka, Z. Árkosi, L. Korecz, Inorg. Chem. 30 (1991) 719–727.
[42] J. Peisach, W.E. Blumberg, Archv. Biochem. Biophys. 165 (1974) 691–708.
[43] A.B.P. Lever, Inorganic Electronic Spectroscopy, second ed., Elsevier, The Netherlands, 1984.
[44] J.P. Scharff, M.R. Páris, Bull. Soc. Chim. Fr. 5 (1967) 1782–1788.
[45] C.V. Banks, R.I. Bystroff, J. Amer. Chem. Soc. 81 (1959) 6153–6158.
[46] A.E. Martell, R.J. Motekaitis, Determination and Use of Stability Constants, second ed., VCH Publishers, Inc., New York, 1992.
[47] G. Anderegg, Helv. Chim. Acta 46 (1963) 2397–2410.
[48] S. Bandyopadhyay, G.N. Mukherjee, M.G.B. Drew, Inorg. Chim. Acta 358 (2005) 3786–3798.
[49] E. Bienvenue, S. Choua, M.-A. Lobo-Recio, C. Marzin, P. Pacheco, P. Seta, G. Tarrago, J. Inorg. Biochem 57 (1995) 157–168.
[50] Z. Árkosi, Z. Paksi, L. Korecz, T. Gajda, B. Henry, A. Rockenbauer, J. Inorg. Biochem. 12 (2004) 1995–2005.
[51] N.A. Roberts, P.A. Robinson, British J. Rheum. 24 (1985) 128–136.